Materials and Design 117 (2017) 305–315

Contents lists available at ScienceDirect

Materials and Design

journal homepage: www.elsevier.com/locate/matdes

Laser diode area melting for high speed additive manufacturing of metallic components

Miguel Zavala-Arredondo [a], Nicholas Boone [b], Jon Willmott [b], David T.D. Childs [b], Pavlo Ivanov [b], Kristian M. Groom [b], Kamran Mumtaz [a,*]

[a] Department of Mechanical Engineering, University of Sheffield, Sheffield S1 3JD, UK
[b] Department of Electronic & Electrical Engineering, University of Sheffield, Sheffield S1 3JD, UK

HIGHLIGHTS

- A novel highly scalable multi-laser powder bed additive manufacturing approach for processing metallic alloys.
- Near full melting of stainless steel alloy powder (99.7% density) using customised low power diode emitters (2.63 W).
- Increased laser absorption and reduced laser power requirement through use of shorter laser wavelength.

GRAPHICAL ABSTRACT

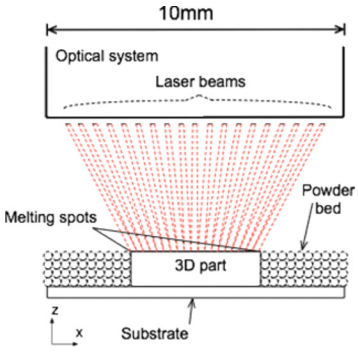

ARTICLE INFO

Article history:
Received 14 September 2016
Received in revised form 14 December 2016
Accepted 31 December 2016
Available online 03 January 2017

Keywords:
Selective laser melting
Additive manufacturing
Direct metal laser sintering
Laser diode
Advanced manufacturing
High speed

ABSTRACT

Additive manufacturing processes have been developed to a stage where they can now be routinely used to manufacture net-shape high-value components. Selective Laser Melting (SLM) comprises of either a single or multiple deflected high energy fibre laser source(s) to raster scan, melt and fuse layers of metallic powdered feedstock. However this deflected laser raster scanning methodology is high cost, energy inefficient and encounters significant limitations on output productivity due to the rate of feedstock melting.

This work details the development of a new additive manufacturing process known as Diode Area Melting (DAM). This process utilises customised architectural arrays of low power laser diode emitters for high speed parallel processing of metallic feedstock. Individually addressable diode emitters are used to selectively melt feedstock from a pre-laid powder bed. The laser diodes operate at shorter laser wavelengths (808 nm) than conventional SLM fibre lasers (1064 nm) theoretically enabling more efficient energy absorption for specific materials. The melting capabilities of the DAM process were tested for low melting point eutectic BiZn2.7 elemental powders and higher temperature pre-alloyed 17-4 stainless steel powder. The process was shown to be capable of fabricating controllable geometric features with evidence of complete melting and fusion between multiple powder layers.

© 2017 The Authors. Published by Elsevier Ltd. This is an open access article under the CC BY license (http://creativecommons.org/licenses/by/4.0/).

1. Background

Additive Manufacturing (AM) is viewed as a disruptive, viable alternative to conventional manufacturing processes, capable of creating

* Corresponding author.
E-mail address: k.mumtaz@sheffield.ac.uk (K. Mumtaz).

http://dx.doi.org/10.1016/j.matdes.2016.12.095
0264-1275/© 2017 The Authors. Published by Elsevier Ltd. This is an open access article under the CC BY license (http://creativecommons.org/licenses/by/4.0/).

geometrically efficient structures with low material wastage. Laser based Selective Laser Melting (SLM) and electron based Electron Beam Melting (EBM) AM systems are increasingly being used in high value sectors to directly manufacture metallic end-use parts from a variety of alloys. During processing, the melting source (deflected laser/electron beam) selectively scans and melts regions of a pre-deposited powder bed. Cross-sections of the part are fused in layers, built up successively to create the complete 3D object. The method of layered fabrication, combined with the high precision of laser melting allows for a greatly expanded design freedom with minimal feedstock waste.

1.1. Capabilities of current metallic powder bed additive manufacturing technologies

SLM or Direct Metal Laser Sintering (DMLS) are considered direct AM processes, capable of fully melting powdered feedstock with the ability to process a variety of metals (steel, nickel, titanium, aluminium alloys) to near full density. A laser spot typically 100 μm in diameter is used to process layers of pre-deposited powder (typically 20–50 μm layer thickness) using laser powers ranging from 100 W–400 W and scanning speeds of up to 2000 mm/s (dependent on material, layer thickness etc.)

SLM systems (e.g. Renishaw, EOS, SLM Solution etc.) typically use a galvo mirror to mechanically deflect a single fibre laser spot (continuous wave or modulated, operating at a laser wavelength of 1.06 μm) over a powder bed along a path that corresponds to the cross-sectional geometry of the component that is being formed [11]. Once a layer has been melted, another thin layer of powder is deposited and the process is repeated until the part has been fully formed. This method of scanning from a single laser source and its reliance on mechanical galvo scanning limits the processing speed of the system. The process can only manufacture as quickly as the laser can be deflected while maintaining a sufficiently high energy density to achieve melting. SLM system manufacturers have attempted to increase system productivity through an increase in laser power (500–1000 W) so that sufficiently high energy densities are achieved as the galvo mirrors deflect the laser beam at a much higher speeds. SLM system manufacturers have also introduced new products that integrate multiple parallel fibre lasers into a single system. The lasers simultaneously scan a powder bed, effectively increasing volumetric build rate. However there are practical space limitations when integrating multiple fibre lasers into a single system (each requiring its own cooling, optics train/galvo mirror etc.). Further to this the cost of the overall system significantly increases when integrating further lasers, including increases in power consumption. Miller et al. have attempted this parallel beam approach for a high-power, multi-beam laser processing system that comprises multiple-independent pairs of selectively rotatable galvo mirrors [15]. However this approach substantially increases equipment cost and energy consumption, with scanning speed still limited by mechanical movement of the multiple galvo systems. Furthermore, the further a laser spot has to travel from the centre of the focusing optic the more likelihood for beam profile deterioration and loss of power, thus there are limits to the area a single deflected laser source can reliable melt.

The EBM process uses the same building principal as SLM, but instead of a fibre laser it uses a high power electron gun (up to 3.5 kW), deflected via magnetism to melt powdered feedstock [18]. The electron gun can be deflected faster than a galvo mirror (electron spot capable of travelling up to 8000 m/s), has a higher power than SLM systems and its electron beam can be split into multiple spots allowing a much faster build rate that SLM (80 cm^3/h EBM compared to 5–20 cm^3/h SLM). However this speed comes at a cost, with the methodology and apparatus used within EBM systems being generally more expensive than SLM systems, limiting its industrial uptake. Furthermore, the surface finish is generally of a poorer quality in EBM, the systems are also known to be more temperamental due to the use of an electron beam melting source.

Present SLM and EBM systems can both be viewed as being inefficient with regards to useful energy conversion (wall-plug efficiency) during the process. The largest contribution to electrical power consumption in SLM is through the laser at 68% [9]. Present state-of-the-art SLM systems are based on fibre lasers, which typically have a wall plug efficiency ~20% [12]. From this, only 20% of the electrical energy consumed by the laser is converted into optical energy. Furthermore, due to general high reflectivity of metals and the laser wavelength operated at, just a fraction of this optical energy will be absorbed and converted to thermal energy during processing. EBM requires a period of substrate preheating prior to layer scanning [14]. Further to this, single layer processing requires three subsequent energy consumption peaks (layer preheating, melting and post melting) making the process inefficient in terms of energy consumption.

Both time and energy consumption are layer-dependant and increase linearly with processed cross-sectional area [1]. It is therefore necessary to reduce both as far as is practical in order to reduce production costs and environmental footprint. A 2012 Innovate UK report on shaping national competency in AM stated that new AM processes needed to be developed that were more cost and energy efficient. The report also stated that one of the main barriers preventing more widespread technology adoption was the slow deposition rates or processing speeds currently available. AM systems need to be developed such that they are 4–10 times faster. A combination of slow build speeds and high SLM/EBM machine depreciation leads to a high cost process [25].

1.2. Development of a high speed efficient additive manufacturing process

The need for speed in manufacturing is clear, parts built faster while maintaining reasonable levels of efficiency enable reduction in manufacturing costs. The need for increased productivity and improved efficiency is an area in which industry has been continually pushing AM system manufacturers and research institutions to make progress. AM is known for its ability to create parts with near zero material waste, encouraging efficient design, and enabling on-demand manufacturing. However, AM is still lacking in its ability to compete with conventional manufacturing for medium to high volume production due to its part fabrication speed. The High Speed Sintering (HSS) process has attempted to tackle this productivity issue within AM by implementing a new approach to processing material from a powder bed [4]. Replacing the conventional laser with the scanning galvo mirror used in polymer Selective Laser Sintering (SLS), HSS is able to significantly increase build speed by using a combination of infrared heating and multiple inkjet nozzles to process larger areas of the powder bed. However due to the low energy density generated by infrared heaters this method is unsuitable for direct processing of most metals. In order to better compete, the limitations imposed by the current SLM system's build methodology and hardware used need to be appreciated and a radical new approach needs to be developed to facilitate melting larger areas of metallic feedstock faster and more efficiently. Fraunhofer ILT have developed a new multi-spot SLM system that does not require galvo mirrors to direct the irradiated laser energy onto a powder bed. Instead it uses a fixed array of multiple laser spots moved on a gantry system of linear axes. These multiple high power laser spots create a controllable intensity distribution to create 3D structures with high flexibility in terms of productivity and building space [6]. However in order for this system to create a single irradiating laser spot, it requires multiple laser diode bars to be stacked/combined with multiple emitters multiplexed to create each of the single 200 W laser spots. Details of exactly how many laser multi-spots have been integrated into this new Fraunhofer machine are unknown, nor has information been released detailing it's processing performance or samples that have been produced.

1.3. Efficient energy absorption through use of diodes lasers

In metals, absorption, A, and reflection, R, of light are directly correlated ($A = 1\text{-}R$). The absorbed light propagates within the material transforming its optical energy into thermal energy. This laser-metal

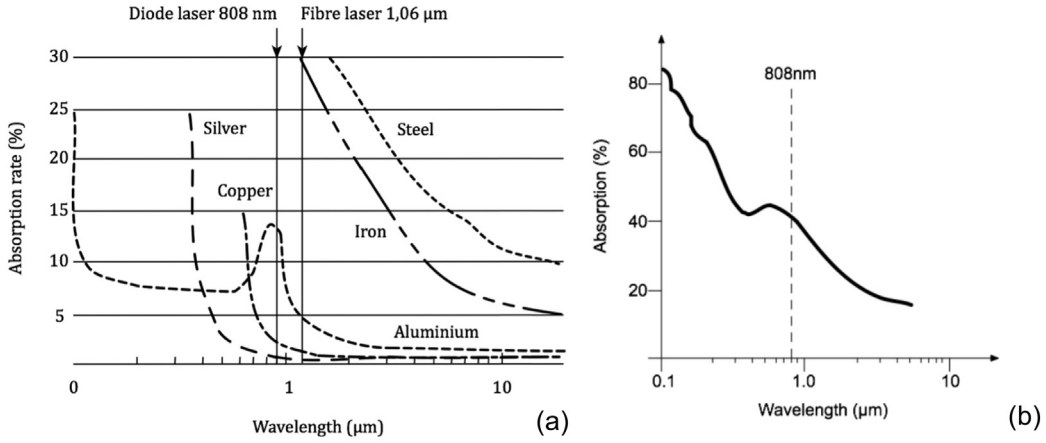

Fig. 1. (a) Theoretical absorption as a function of wavelength for a range of common metals, adapted [3] and (b) specifically iron, adapted [20].

interaction is crucial for determining the laser melting efficiency of metallic powder. Fig. 1(a) plots the absorption rate of a number of common metals as a function of the wavelength of irradiation. In metals, short laser wavelengths within the infrared spectrum typically result in higher laser absorption [3]. The laser wavelength of conventional SLM equipment (usually 1.06 μm) limits the laser absorption of the metallic particles requiring higher laser powers to melt and therefore increasing energy consumption. For example, aluminium benefits from a ~3× increase in absorption with a reduction in wavelength from 1.06 μm to 808 nm as shown in Fig. 1. Increases in a materials' ability to absorb energy with a shortening of wavelength is also seen for other elements such as copper, silver and iron (Fig. 1(b)).

Diode Lasers (DLs) are some of the most efficient devices in converting electrical into optical energy, working at wall plug efficiencies up to 50–80% [12]. The ability to tune the emission wavelength of DLs through choice of semiconductor active material allows DLs to be designed or selected to match the peak absorption wavelength of the powder material being irradiated. High-power DLs are typically used for laser pumping of solid-state lasers where they are packaged in dense arrays and as the input for fibre-optic direct-diode laser devices among other applications [7]. DLs are gaining popularity in direct material processing applications such as surface heating and welding, where performance improvements have been demonstrated such as more uniform melt and heating zones, greater consistency and repeatability [5]. Unfocused diode laser beams are also used to assist pulsed laser welding on aluminium due to their higher absorption. Materials processed using diode lasers have demonstrated more uniform melt and heating zones which resulted in fewer cracks being incorporated into the weld zone compared to Nd:YAG and CO_2 lasers [13]. The expansion of formed melt pools can be conduction limited, however when temperatures are high enough to cause material vaporisation, keyhole melting may occur allowing the laser to more deeply penetrate the processed material [10]. DL arrays can be stacked horizontally or vertically, be actively cooled and their beams combined to realise kW powers.

High-power DL arrays can be sourced operating at 808 nm where they are commonly used for pumping Nd:YAG lasers. A schematic diagram representing one such module is shown in Fig. 2, annotated with the specifications of the module used in this study (A 50 W output power 808 nm wavelength bar mounted on a standard CS-mount, comprising 19 × 135 μm wide emitters with a 500 μm period). The emission of such arrays is typically divergent to the tune of ~30–40° in the vertical

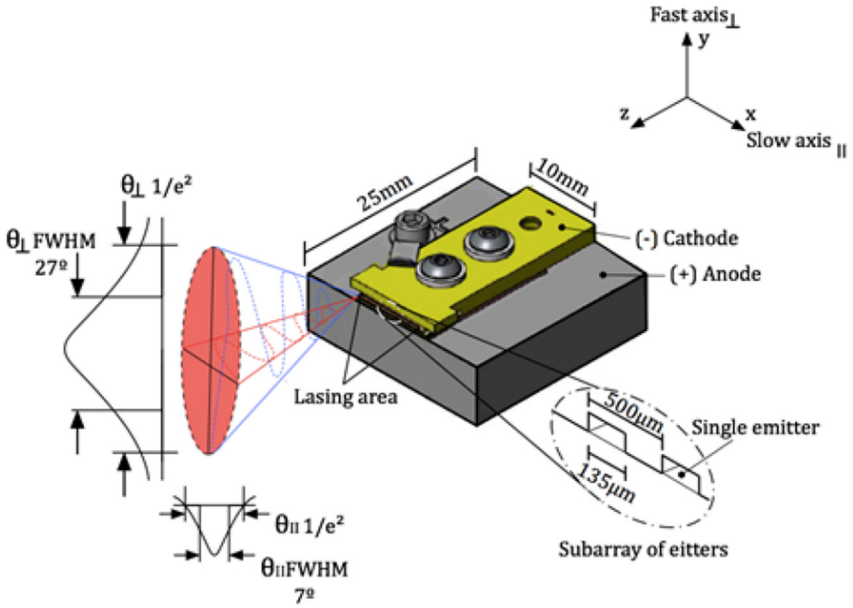

Fig. 2. Standard diode laser bar with 19 emitters. Emitter width of 135 μm on a 500 μm pitch. The divergent emission from one such emitter is pictured, with divergence of 27° (fast-axis) and 7° (slow-axis) [19].

direction (fast axis). This can be corrected using collimating micro-optic lenses attached to the front of modules, resulting in a stripe of radiation that can be used for pumping solid state laser rods. However, the stripe-shaped output from standard DL arrays is not directly suitable for processing net shaped parts.

The high divergence of DLs in the fast-axis (FWHM of 27°) is combined with a smaller (FWHM of 7°) divergence in the horizontal (slow-axis) direction. FWHM (Full Width at Half Maximum) refers to the half width of the optical far-field of the divergent beam (see Fig. 2). The large asymmetry of the elliptical beam emitted from each laser in the array necessitates the application of both a Fast-Axis cylindrical Collimating lens (FAC) and a Slow-Axis Collimating (SAC) cylindrical micro-lens array [23,26]. Short focal length lenses are also required for collimation and focusing respectively [8]. A real beam that does not exhibit a perfect Gaussian distribution is said to be M^2 times diffraction-limited. Collimated diode laser beams usually have an M^2 ranging from 1.1–1.7. High-energy multimode DLs can have M^2 as high as 20 to 50 [22]. Multimode DLs are used in cases where a large amount of power is needed. For this, multiple emitters can be stacked in a single module.

2. Diode area melting methodology and system development

The limitations of single/multiple deflected lasers based on a 1.06 μm fibre laser used in SLM has been identified. A replacement of this single point energy source and a rethink of the scanning methodology used to melt material is a first step in tackling the limitations of melting speed experienced by SLM. As detailed in Section 1.2, Fraunhofer ILT have made progress in tackling these SLM limitations by developing a multi-spot laser system. To create each individual laser spot, Fraunhofer's system is required to combine stacks of diode bar arrays comprising of many emitters multiplexed into a high power laser spot [6]. Use of more direct approaches (i.e. use of non-multiplexed laser sources) where one diode emitter is used to irradiate a single laser spot directly onto a powder bed has not yet been reported.

The Diode Area Melting (DAM) method replaces the deflected fibre laser used within SLM with multiple emitters co-located within a customised DL bar (shown in Fig. 3). Each customised bar contains an array of individually addressable emitters each with collimating micro-optics built onto the module, and further focused through a pair of cylindrical lenses to irradiate the powder bed with a linear array of independently controlled laser spots, each with an elliptical shape. The optics can be controlled to allow an overlapping of the individual beams in order to create a continuous high-power stripe, such as is necessary for large area melting of high melting point materials. The multiple emitters of the bar (emitter spacing at the facet is 0.5 mm) overlap along the x-axis to produce an area of high energy density able to melt the powder bed. These customised bars will have their individual emitters electrically pumped independently to activate them (turn on/off). The DL bar traverses across the powder bed with the emitters turning on/off as required to selectively melt regions of the powder bed. The individual laser spots generated by the DL bar are not deflected as those used in SLM to create a shape, but are instead activated to form a vertical beam to create features while the DL/substrate traverses. This process may be likened to multiple nozzles within an inkjet printhead, printing or irradiating over areas that correspond to the geometry to be printed/formed. DL bars are highly compact compared to fibre lasers and are therefore scalable such that multiple arrays could be stacked, enabling large areas of a powder bed to be irradiated at rates higher than that of a single point laser source. The key theoretical benefits of using individual non-multiplexed diode emitters to create multiple laser spots on a powder bed are summarised in Table 1.

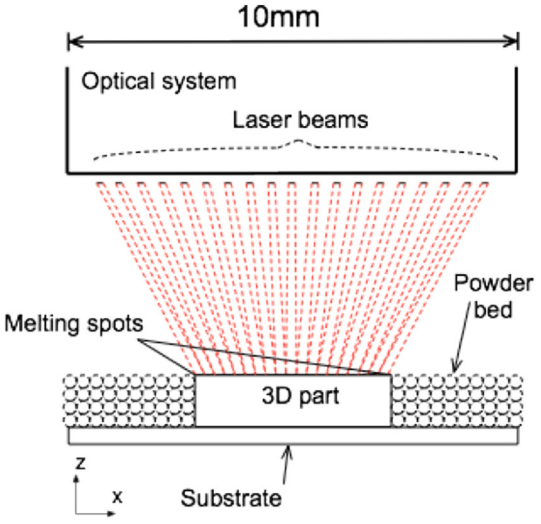

Fig. 3. Diode Area Melting, individually controllable emitters within moving diode laser bar selectively turn on/off to melt shape over powder bed (additional corrective focussing lenses not included for simplicity).

2.1. Fully integrated diode area melting test rig

The developed DAM system is enclosed within a custom chamber that is pumped with argon gas during processing (oxygen concentration in the chamber is reduced to < 1000 ppm before processing). In the present embodiment, the DL modules bars, which are thermoelectrically cooled, remain stationary during processing whilst the powder bed is traversed. However, a scheme is also possible where the modules themselves are traversed. In addition to FAC/SAC collimation, two additional plano-convex lenses were aligned to the fast and slow axis respectively to focus light in the parallel and perpendicular directions. An inert gas air knife also passes just above the processing table to prevent contaminants during processing from adhering to the focusing lens or reaching the laser facets. A motorised bed processing table (controlled by LabVIEW) adjustable in the x and z axes is positioned directly below the focusing optics for the lasers (Fig. 4). The enclosed chamber is a two glove glovebox, to allow for manual deposition of powders after each processing scan.

Table 1
key theoretical benefits of diode area melting.

DAM	Current SLM technology	DAM benefit
Array of independently addressable diode laser emitters.	Galvo scanning of a single fibre laser beam.	Faster build speed, smaller laser unit size, lower cost, compact stackability of multiple lasers.
Possible spot size reduction.	Minimum spot size limited by numerical aperture of fibre and lens	High resolution enabled by small focussed spot size in the array
Scalability to large scanning areas.	Speed penalty for rastering over large parts. Space limited.	High speed maintained for large parts. Not space limited.
High 50–80% wall plug efficiency laser.	20% wall plug efficiency of laser.	Greater electrical to optical energy efficiency.
Tuneable wavelength to peak absorption of material, multi-materials.	Single wavelength high-power laser.	Greater melting efficiency, greater functionality. Functionality
Optical preheat.	Substrate heating, RF heating.	Precise, fast surface heating.
Future application of 2D VCSEL/PCSEL arrays.		Remove need for any scanning.

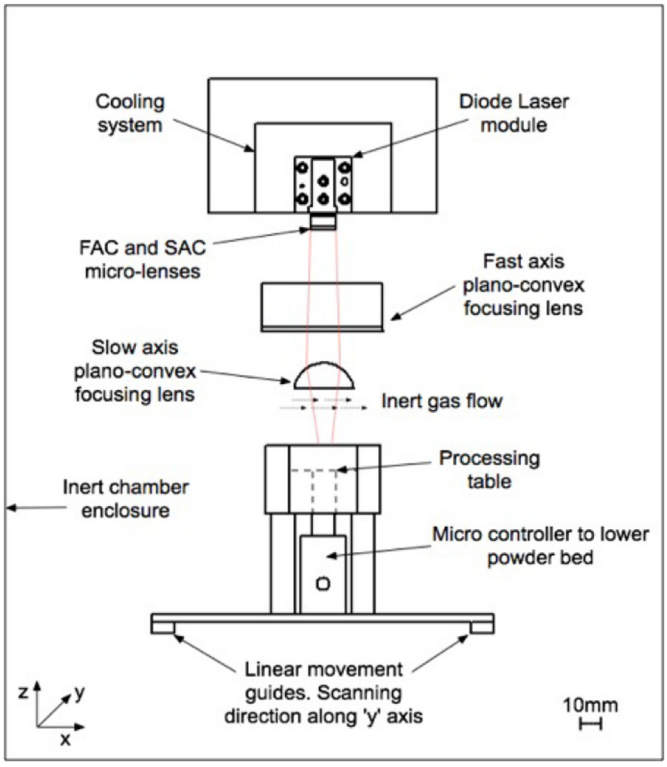

Fig. 4. Diode area melting test rig key components.

2.2. Customised 808 nm diode laser bar control and beam profile measurement

The DL bars (continuous array of 19 lasers) used in the DAM system were sourced from Oclaro (now II-VI Laser Enterprise, Zurich) and emit laser radiation at a wavelength of 808 nm. The maximum power output of the CS-mounted module is 50 W spread over the 19 emitters (i.e. each emitter can contribute 2.63 W). In this laser bar, the 19 emitters are 135 μm wide with 500 μm period. FAC and SAC collimation optics are mounted to the output facet of the bar to collimate the individual beams. The use of SAC optics in particular allows individual beams originating from the individual emitters in the bar to remain separated prior to focusing onto the powder bed. LabView was used to control the individual emitters and the stepper motor attached to the powder bed stage such that selective melting and feature creation could be controlled along the y-axis.

In order to make the 19 emitters individually addressable for net-shaping capabilities, the individual lead-outs from each emitter needed be independently operated. In order to achieve this level of customisation, a dual-beam Focused Ion Beam (FIB) system was used to mill the metal layer connecting individual devices (since common usage of such bars operates all lasers simultaneously). The FIB system comprises a JEOL 6500F scanning electron microscope (SEM) with an Orsay Physics Ga + ion column, which focuses the ion beam to a submicron spot size to mill material in the exposed area. A milling current of 0.16 nA and a beam energy of 30 kV were used. Electrical pumping was provided by a Thorlabs PRO-8000 multiple current source to power and control each emitter.

The optical beam profile of the 19 emitters working together at a focal distance equivalent to the distance between the slow axis focusing lens and the powder bed was measured using an opal glass target from which the melting beam area was projected and recorded using a Spiricon camera based beam profiler (BeamMic Software was used to measure the beam dimensions). Fig. 5(a) shows the beam profile at the facet of the diode bar after micro lens collimation of the emission of all 19 lasers and before focusing. The fast axis (2.5–6 times more divergent than the slow axis) collimation will determine the minimum spot dimensions and is the first to shape the beam. After collimation, cylindrical plano-convex lenses were used to focus beams and reduce the separation between spots. The focused beam profile shown in Fig. 5(b) covers a width of 4.5 mm and demonstrates superposition among adjacent spots, as is required to achieve high energy density across a continuous area. The melt width is limited due to the experimental setup consisting of only one diode bar with 19 emitters. Extension and upscaling of this melt width over the powder bed would require multiple-stacks of these diode bars to be connected end-to-end.

3. Experimental methodology

To determine the melting capabilities of the DAM system the temperature profiles for both BiZn2.7 and Stainless Steel 17-4powder was measured at the surface of the powder at variable laser powers and processing speeds. The geometric forming capabilities were tested as individual emitters were activated to melt powdered feedstock. The density of DAM processed BiZn2.7 and Stainless Steel 17-4 formed components were analysed to determine whether a sufficient thermal energy density had been generated to achieve full melting of powdered feedstocks.

Initially a low temperature eutectic composition of BiZn2.7 was used to test the melting capabilities of the DAM system. Bismuth (with a melting point of 271.442 °C) was elementally mixed with a higher melting point zinc powder (470 °C). This composition was successfully processed to high density (>99%) using conventional SLM trials and represents a low temperature SLM candidate material [17]. Bismuth powder (sourced from Acros Organics with D50 of 149 μm) and Zinc

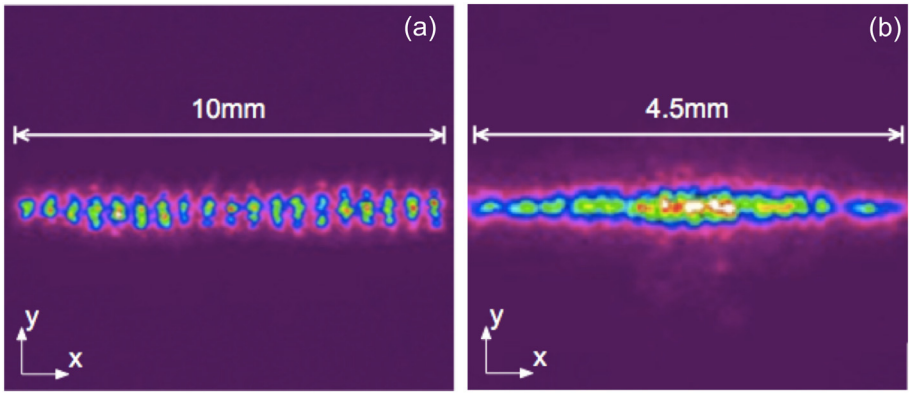

Fig. 5. Beam profile measured using a Spiricon camera based beam profiler and BeamMic software; (a) output from all 19 DL emitters at the facet (before focusing), operating simultaneously at 2.63 W each; (b) beam profile of the 19 emitters focused to a single stripe of overlapped spots.

Table 2
Scanning velocities and energy densities generated during DAM processing.

Scanning velocity (mm/s)	Energy density (J/mm^3)
0.5	83
1	42
3	14
5	8

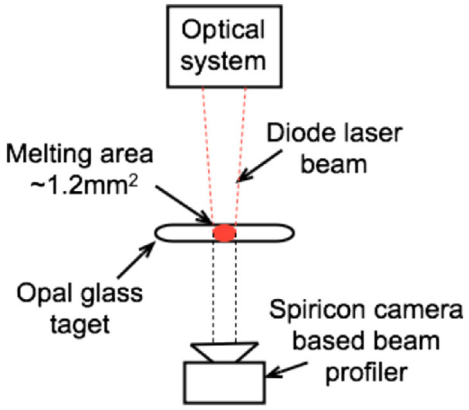

Fig. 6. (a) Laser profiler methodology.

particles (sourced from Fisher Scientific with D50 of 100 μm) were weighed and mixed in specific percentages and deposited onto a 25 × 25 mm BiZn2.7 substrate. The powders were manufactured by mechanical grinding and therefore had an irregular shaped morphology and broad size distribution. The large particle size of the powders prevented layers of <200 μm from being deposited.

Stainless Steel 17-4 powder (sourced by EOS; D50 of 50 μm) was used for processing high melting point materials using the DAM system. Due to the manual deposition of 17-4 powders, minimum layer thickness was limited to 150 μm. For a powder bed metal AM process this is far thicker than would normally be used as a layer thickness (SLM normally uses 30–50 μm). For both BiZn2.7 and Stainless Steel 17-4, varying scan speeds were investigated, ranging between 0.5 and 5 mm/s at the maximum power of 50 W over the entire DL.

3.1. Temperature transient measurement

A Flir 9 Hz thermal imaging camera was initially used to measure the temperature transients with a set value for emissivity of material being processed. However when this proved too slow to capture temperature rises due to rapid absorption and conduction of heat a secondary rapid high speed measurement system was used. By fitting a Hamamatsu C11440-22CU with an f/1.4 lens and an RG850 850 nm high pass coloured glass filter, the camera could operate as an infrared imager and produce thermal images once calibrated. The camera was calibrated against a LANDCAL R1500T blackbody temperature reference, which was itself previously calibrated to a UKAS temperature transfer standard.

3.2. Density measurement

DAM processed BiZn and Stainless Steel 17-4 samples were cross-sectioned through multiple layers (along z-axis build height), mounted and polished. The level of porosity in the specimen was determined and estimated by area fraction analysis of representative micrographs/fields using a method based on ASTM E2109-01 (2007) and BS 7590:1992.

4. Results and discussion

Temperature transients were measured at the surface of the process powder bed for both low and high temperature metallic powders (BiZn2.7 and Stainless Steel 17-4) at varying process speeds in order to determine the maximum temperature achieved in each case. Also the shape forming capabilities of the DAM process are discussed, in addition to density analysis of DAM-formed BiZn2.7 and Stainless Steel 17-4 components.

4.1. Temperature transient - low melting point BiZn2.7 powder

Multiple energy densities were generated through varying the scan speed with all emitters operating at maximum power (2.63 W each, 50 W for the entire DL array) shown in Table 2. To calculate the energy density, the focused beam profile from Fig. 5b was analysed using a Spiricon camera based beam profiler and an opal glass target as depicted in Fig. 6a. The area under the superimposed beam was calculated to be 1.2 mm^2. The beam is projected onto the opal glass and then recorded by the profiler.

The total power used in the calculations was the diode bar maximum output power of 50 W. The energy density for the entire melting area can be calculated using Eq. 1, with the scanning velocities used given in Table 2.

$$\text{Energy density}\left(\frac{\text{J}}{\text{mm}^3}\right) = \frac{\text{Laser power (W)}}{\text{Scanning velocity}\left(\frac{\text{mm}}{\text{s}}\right) \times \text{Area}(\text{mm}^2)} \quad (1)$$

The maximum temperature over a 25 × 25 mm area over a ~0.2 mm thick BiZn2.7 powder bed was measured with the Flir 9 Hz thermal imaging camera as shown in Fig. 7a. The emissivity ε = 0.67 was predicted using Sih and Barlow method for emissivity in powder beds[24]. The temperature transient was measured on a moving powder bed at the different scanning speeds shown in Table 2. In Fig. 7b, the actual melting beam of 19 focused diode laser emitters on BiZn2.7 powder bed is shown.

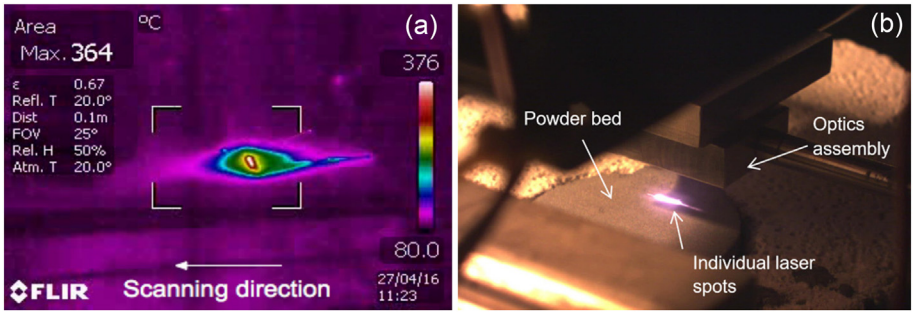

Fig. 7. (a) Temperature distribution over 25 × 25 mm area during DAM processing of BiZn2.7. (b) Shows the actual melting beam of the diode bar on the powder bed.

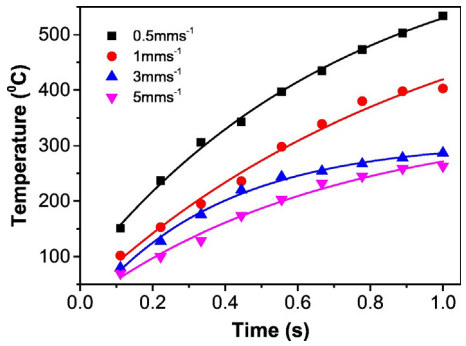

Fig. 8. Temperature transients of Diode Area Melted Bi-Zn2.7, measured for a range of scan speeds.

Fig. 8 plots the temperature transient measured for a range of scan speeds with the full DL array operating at the maximum 50 W. The temperature at the surface of the powder rises quickly, with the speed of this rise being dependent upon the scan speed. Higher temperatures are achieved faster at slower scan speeds as a result of higher energy densities being generated. The maximum unalloyed melt temperature of a BiZn elemental mix is 420 °C (zinc's melting temperature). This temperature was reached at the surface with a scan speed of 0.5 mm/s after approximately 0.6 s with an energy density of 85 J/mm^3. With faster scan speeds the maximum temperature measured within the 25 × 25 mm area was below the melting temperature of zinc and therefore deemed unsuitable for complete melting of BiZn2.7. After 1 s the maximum temperatures were attained and stabilised due to a constantly moving laser beam.

4.2. Diode area melting shaping capabilities

The capability to create shaped parts was investigated using the processing parameters determined in Section 4.1, which proved capable of generating powder surface temperatures above 420 °C (identified in Section 4.1). Individual emitters across the DL were activated to create specific shapes. However when high energy densities were used (above 40 J/mm^3 to process BiZn, significant overmelting would occur leading to difficulties in depositing further layers. An energy density of 30 J/mm^3 was found capable of sufficiently melting BiZn powder without significant overmelting and powder deposition issues. Fig. 9 shows the scanning patterns and processed geometries created by activating 4 emitters while generating an energy density of 30 J/mm^3 across the BiZn2.7 powder bed using a single scanning path. The red and grey circles in the schematic diagrams represent the ON and OFF state of individual emitters, respectively, while traversing the powder bed under the DL. Features can clearly be seen within the processed powder bed that correspond to the emitter activation scan strategy. The samples were created from ten ~200 μm BiZn2.7 layers. Despite the theoretical width of the melting area being ~1 mm, covered by 4 emitters (19 emitters covered an elliptical melting area of 4.5 mm width in Fig. 6b, therefore each emitter should cover ~0.24 mm width considering overlap) the features created measure >2 mm. This may be a result of larger melt pools being formed due to bismuth's low melt temperature of (270 °C) making up the majority of the BiZn2.7 feedstock. During processing, a laser-induced surface temperature profile reaching in excess of 500 °C (Fig. 7) was created within 1 s. This would have led to a potential overheating of the feedstock (combined with a low scan speed) causing the melt pool emanating from the centre of the laser spot to rapidly expand, creating larger features.

4.3. BiZn2.7 part density

The DAM processed BiZn2.7 samples were cross-sectioned across the z-axis (across the build height) in three locations along its length, then mounted, polished and their average density measured. Fig. 10 shows an optical cross-sectional micrograph of a DAM built BiZn2.7 sample. The cross-section exhibits a number of irregular shaped pores. However, the samples have a high overall average density of 99.27%. The observed porosity was attributed to the thick ~200 μm layers that form the powder bed and inconsistencies associated with the manual process used for its deposition resulting in non-uniform melting.

The top surface of the samples were not completely flat, this may have been due to inconsistencies during the manual deposition of powders. The sides of the samples were not completely uniform nor smooth, displaying signs of satellite formation and excess balling (track instabilities, the breakup of molten material into smaller entities in order to break up surface tension, most likely caused by the thick layer deposition or material being held in a molten state for too long (the melt pool will subsequently break up using the balling mechanism in order to reduce its excess surface free energy) [16].

With conventional SLM, scanning paths for features larger than a single scan typically consist of overlapping laser scans so that porosity is minimised. The DAM system's overlap between emitter spots cannot be adjusted without a hardware modification. The position of each spot along a parallel scan line is fixed by the spacing between lasers in the DL bar and setting of the optics used in the system (de-focusing permits adjacent overlap of emitters). An alternative to hardware adjustment to combat insufficient melting in between emitters (due to insufficient overlap), the laser power may be increased or scan speeds reduced such that the melt pool or heat affected zone is expanded so that pores between emitters can be reduced. The bismuth and zinc powders used within experimentation were irregular shaped, this would reduce the powder bed packing density increase the likelihood of pores being present. A reduction in powder layer thickness and use of a powder with a spherical morphology and lower particle size may have assisted in reducing overall sample porosity.

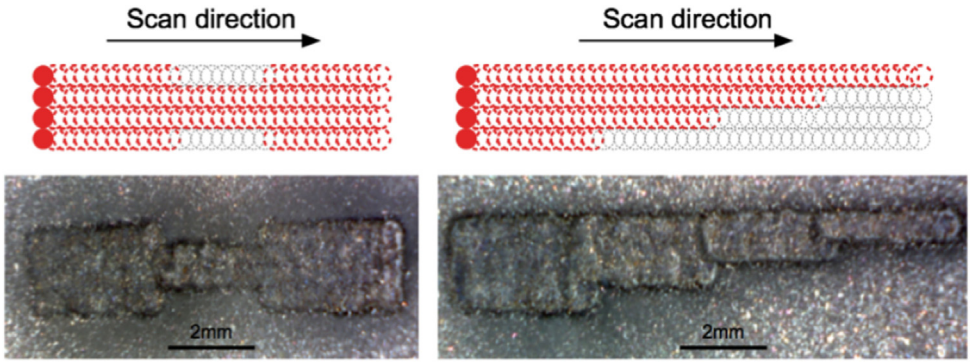

Fig. 9. 2D patterns creating using 4 individually addressable emitters from a customised DL module for Diode Area Melting.

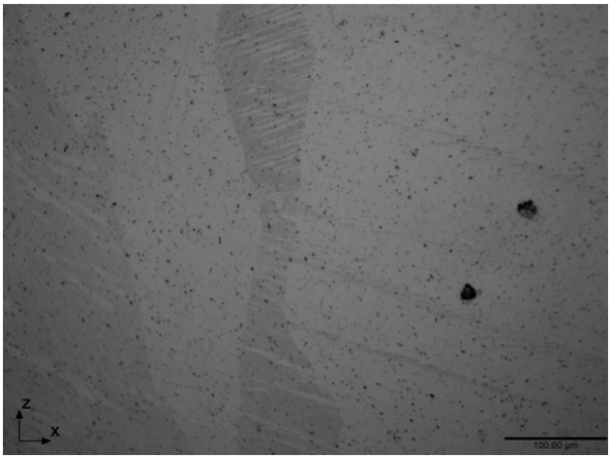

Fig. 10. Cross-section of Diode Area Melted BiZn2.7, samples contained some irregular shaped pores, whilst attaining a maximum density of 99.27%.

4.4. Temperature transients - Stainless Steel 17-4 powder

The same DAM process parameters applied in Section 3.1 were used to measure surface temperature profiles on a 150 μm thick Stainless Steel 17-4 powder bed. Due to the rapid heat absorption/conduction of Stainless Steel 17-4 the Flir 9 Hz thermal imaging camera was unable to accurately measure the temperature at the surface of the powder. Instead a Hamamatsu C11440-22CU camera was used, its specifications are detailed in Section 3.1. The calibration procedure for the camera involved taking a series of measurements with the camera over the temperature range required (600–1450 °C). A curve was then fit to this data to produce a brightness to temperature conversion scale for the image data. As the camera was calibrated against a blackbody source with an emissivity $\varepsilon = 0.99$, any images captured would need to take this into account as the emissivity of the surface being imaged is likely to be lower. To calculate the emissivity of the surface a method from Sih & Barlow was used [21]. This took into account the emissivity of the solid material and the porosity of the powder in use; producing an emissivity for the powder bed. The porosity of the powder was measured at 0.2192 and the solid emissivity of a similar steel alloy was found to be 0.44 (the solid emissivity used was that of a closely matching alloy 17-4). This lead to $\varepsilon = 0.4754$ for the bed as a whole. This value was used as a multiplier for the brightness data in the images, therefore correcting for extra reflected radiation versus the high emissivity source used for calibration. To acquire the images, the camera was run in its high speed capture mode at a resolution of 64 × 2048, this allows images to be acquired reliably at 900 frames per second. The camera was set to a 1.101 ms integration time to keep this constant with the calibration. Images were streamed to a PC where they were saved as TIFF files for later processing. This was done in MATLAB and consisted of cropping the images to the region of interest around the laser, then performing the conversion to thermal images using the lookup table produced in the camera calibration process. The result was a series of images with each pixel value representing a temperature in degrees Celsius shown in Fig. 11.

Fig. 12 plots the measured temperature transients obtained for a range of scan speeds with maximum 50 W operating over 19 emitters (Table 2 shows the processing parameters used). The temperature rise for all scan speeds are rapid, with temperature exceeding 1300 °C within 6 ms for each scan speed used. After this period the camera was unable to record the temperature (due to image saturation). According to Fig. 1(b), the laser absorption of Iron (which comprises ~70% of 17–4 powder composition) at 808 nm wavelength is above 40%. This high level of absorption is expected to rise as the temperature of the formed melt pool increases [2]. The recorded temperature is still below the

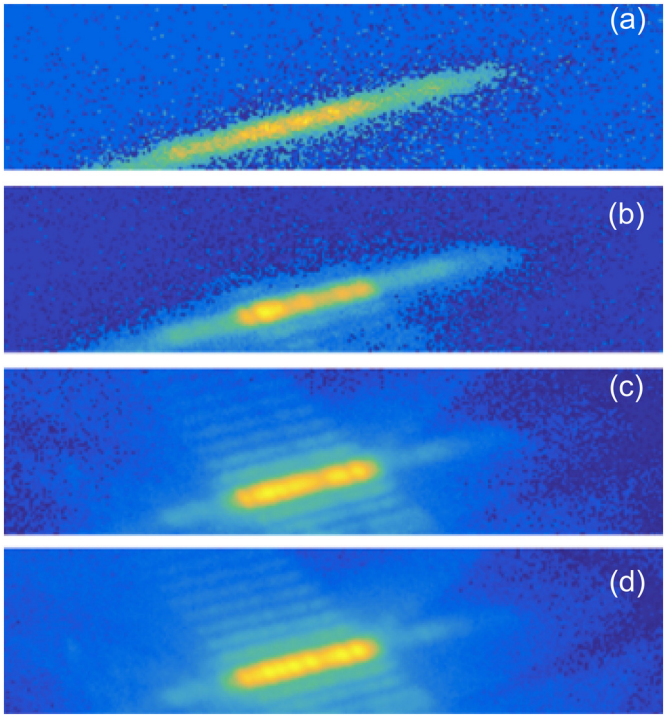

Fig. 11. Thermal imaging measurements of Stainless Steel 17-4 at 900 frames per second during Diode Area Melting. Images from a to d correspond to subsequent frames from full DL activation to melting.

melting point of 17-4, however due to saturation of the recorded images after 6 ms it is still unknown whether higher temperatures were reached. This can be determined during DAM processing of 17-4 with density analysis. Due to the calibration range/dynamic range of the camera, only wavelengths corresponding to a temperature range of 500 °C to 1350 °C were observed in a 4 frames range starting from 2 ms to 6 ms.

4.5. Stainless steel 17-4 part density

Due to the spherical morphology of the 17-4 powder and relatively fine particle size (D50 of 50 μm) compared to the BiZn2.7 feedstock (D50 of 149 μm) it is theoretically possible to deposit thinner layers and thereby reduce the amount of energy required to melt a layer. However due to the manual method used to deposit powder layers, it was not possible to accurately deposit layers thinner than 150 μm, again this is ×3 thicker than what would normally be deposited using

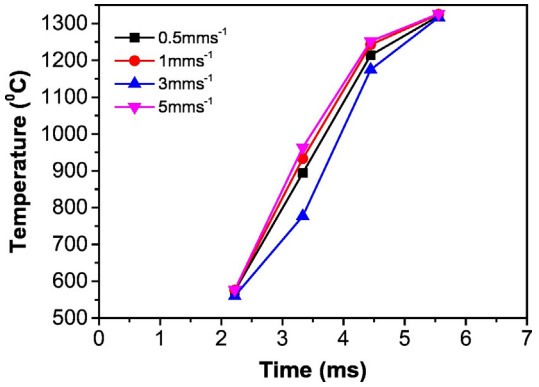

Fig. 12. Temperature transient of stainless steel 17-4 process using Diode Area Melting. Each point corresponds to a single frame from Fig. 10. The connecting line between points is a guide for the eye. Camera sensitive for wavelengths corresponding to a temperature range 500 to 1350 °C.

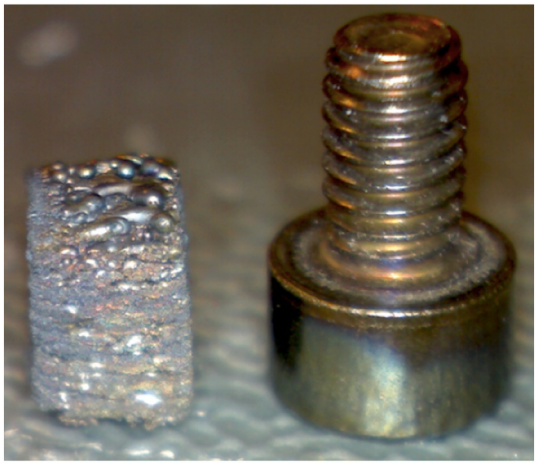

Fig. 13. Diode area melted 17-4 component (left), adjacent to an M4 bolt.

conventional SLM. With all 19 emitters activated, a cube structure measuring ~4.5 × 4.5 × 6 mm was formed from 40 × 150 μm thick layers, a single scanning path was used for each layer. To maximise energy density (83 J/mm^3) and achieve a high part density a scan speed of 0.5 mm/s was selected, with output power set to the maximum 50 W operating across the DL array. An image of the component formed by this process is shown in Fig. 13, positioned adjacent to an M4 bolt scale visualisation. The component is solid and can be removed/handled from the stainless steel substrate plate. Part geometric distortion can be seen, it exhibits irregularities at the surface and high surface roughness. The geometric distortion (i.e. bowing vertical surfaces) is most likely the result of employing a manual non-optimised powder deposition approach combined with general inaccuracies related to the system x-y table and perhaps beam path distortion due to heating of the DL bar. The surface irregularities (bulging at top surface) may be a result of slow scan speeds creating a melt pool that continues to grow and draws in feedstock material that surrounds the melt pool, creating peaks and troughs of melted material. Deposition of thicker powder layers will amplify this issue further. The high sidewall surface roughness is a result of the large layer thickness and potential satellite formations. These are partially attached surrounding powder particles that were unable to completely enter the melt pool, but rather neck or partially sinter to the outside of the solidified melt pool, creating a high side surface roughness. Periodically along the build height a defined interface between layers can be seen, this would suggest that layers had not completely melted during DAM.

Fig. 14 shows an optical microscope image of the cross-section of the 17-4 sample (across the build layers). The image contains regions indicative of a lack of fusion between layers. Such levels of porosity appeared to occur randomly across the component's cross-section. This randomness may be attributed to a number of different factors, these include; inconsistencies in powder layer deposition (due to manual deposition), progressive blocking of laser beam as lenses become dirty during processing, continual rise and fall of laser diode temperature affecting beam alignment. These potential processing issues and inconsistencies in part density, geometric integrity and surface finish can be identified/excluded through further system development/optimisation (i.e use of automated powder depositing system, reducing layer thickness, further optimisation of processing parameters etc.). Within the sample there were large sections of melted 17-4 with z-axis solid non-porous features in excess of the 150 μm layer thickness, with some features measuring 600 μm across the z-axis. This clearly shows that despite there being a clear lack of fusion between some regions/layers, there is evidence of multiple thick layers being successfully fused within other regions of the sample (see Fig. 15). In these areas an average density of ~99.72% was attained. Such densities are comparable to conventional SLM technologies. Within these regions there was no evidence to suggest that there was insufficient energy density to melt multiple 150 μm thick 17-4 powder layers. There existed within these regions spherical micro-pores that may be associated with gas occluded porosity (present within the gaps between the power particles or gas already existing within the powder particles themselves). The density of the entire 4.5 × 4.5 × 6 mm component (porous and dense areas together) was calculated to be ~79.18%.

The ability to successfully melt large areas of a powder bed in a single pass, from thick multiple layers of a material with melting temperature in excess of 1400 °C is encouraging. This outcome, from what would conventionally be conceived to be an underpowered energy source (2.63 W for laser), was able to achieve melting through use of a relatively low power and efficient (compared to diode pumped solid state or fibre laser) diode laser and focusing optics. There are clearly issues with randomised high levels of porosity inclusions within the component and high surface roughness with geometric distortions. These issues are likely to be linked to the non-optimised early stage setup of the current DAM system, use of manual powder layer deposition, undesirably thick layer deposition, issues with non-perfectly aligned focusing optics, and overlap between laser spots. Further to this, cooling units for the DL heatsinks are non-optimal (air cooled rather than water cooled), temperature rises due to prolonged use will affect the consistency of the DL beam quality. The further development of this early stage process will increase knowledge surrounding these processing issues and facilitate improvement in part quality

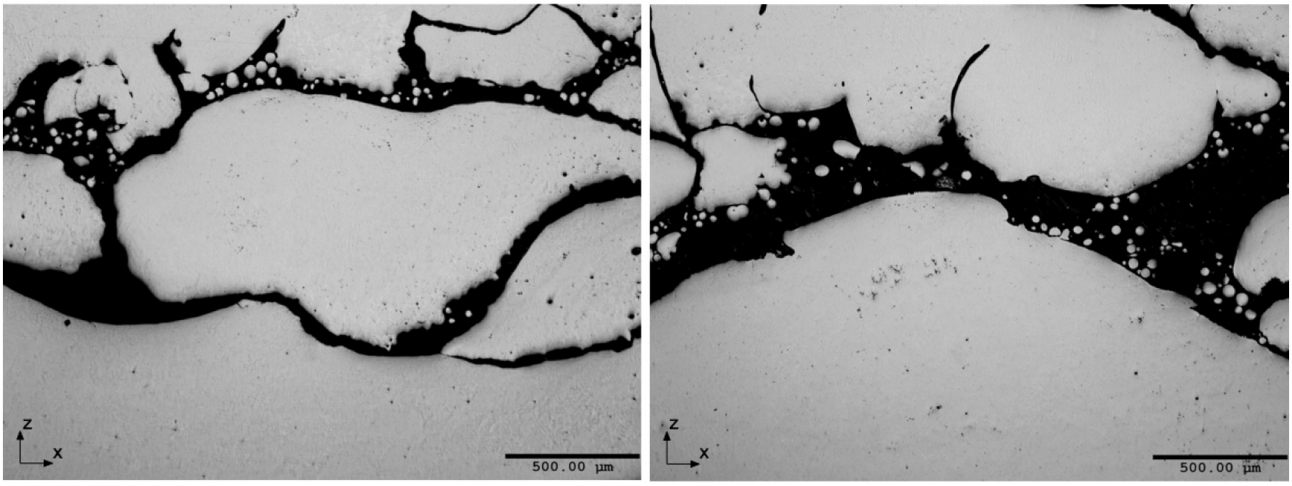

Fig. 14. Areas displaying lack of fusion across layers (~80.76% average density).

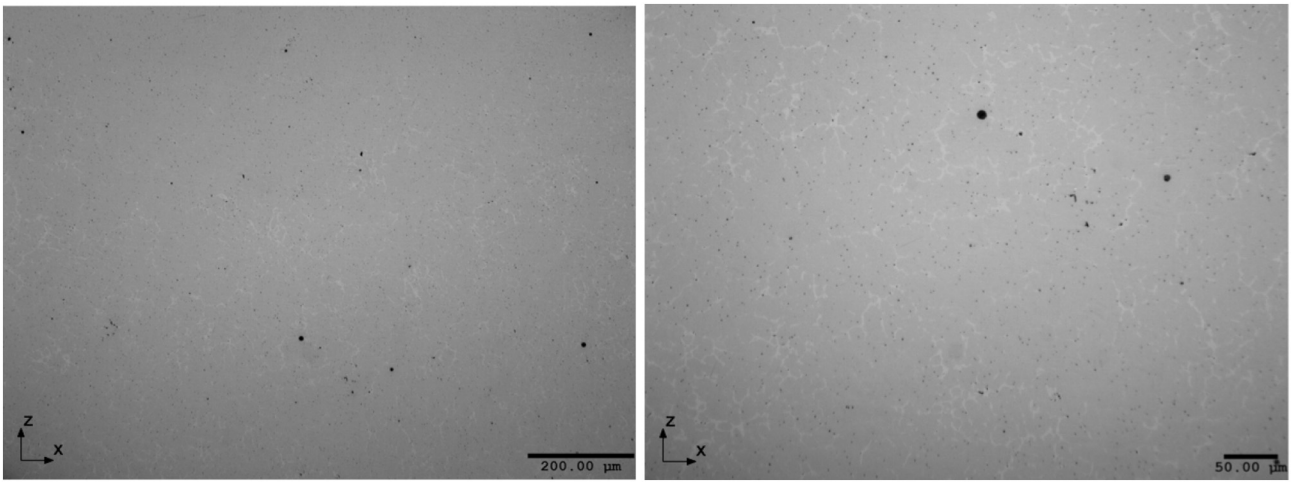

Fig. 15. Areas displaying high density and successful diode area melting across multiple layers (~99.72% dense).

5. Conclusions and key novelties of diode area melting

A new methodology and system has been presented for additive manufacturing of metallic components. The traditional galvo scanning methodology used within a single fibre laser SLM system has been replaced with arrays of multiple individually addressable and non-deflected low power diode laser beams in order to scan in parallel, selectively melting material from a powder bed. The ability to near-net shape and process material with melt temperatures in excess of 1400 °C from a lower power source presents the greatest challenge. This work demonstrates the potential in harnessing the theoretically efficient absorption characteristics of these low power diode laser bars to generate sufficient energy density to melt engineering grade materials. The DAM process was able to successfully fuse multiple ~150 μm thick layers of stainless steel 17-4 powder, attaining ~99.72% density in specific areas within the 3D formed component. However, due to the process being in an early stage of its development, it is considered to be a far from optimised system (e.g. optics, cooling), relying on manual layer deposition of thick powder layers from which part defects can form (i.e. geometric distortion, high surface roughness and randomised high levels of porosity within components). These component quality issues can be alleviated through further process optimisation and control.

The difficulties presented in the integration of diode lasers into the DAM system include the focusing of divergent beams into tight stripes. High numerical aperture lenses are needed to achieve the energy densities required to melt metallic particles. This makes the superposing alignment a challenge. Improved design of the DAM's optical system may produce higher energy density beams capable of melting at a lower laser power. However, reduced focusing space may be a constant challenge for melting with low powered diode emitters. In future developments the manual powder deposition should be developed into an automated process (as with conventional SLM/EBM) with finer more consistent layer deposits (~50 μm), thus requiring less energy to melt the feedstock material and will enable a speeding up of the DL scan over the surface of the powder bed. Thinner layers will reduce surface roughness and may alleviate the tendencies for the melt pool to break up into smaller entities (balling formation).

In parallel to process development, new materials can be explored for DAM processing potential. Multi-materials can be processed at different laser wavelengths (multiple different-wavelength diode emitters working together) to match multiple peak absorptions, opening the possibility of improved control of alloying. Aluminium has an absorption peak located close to the operating wavelength of the DL used within this work. Aluminium is a challenging material to process even with conventional SLM due to high reflectivity/conduction and high oxidation potential, often requiring very high energy densities to achieve full part density. However DAM may be able to overcome these higher energy requirements by operating at a more efficient laser wavelength and reduce the power required by the laser to melt the material by introducing powder bed pre-heating and/or a new optical surface pre-heating. Optical pre-heating would be highly suited to DL due to their high beam divergence. DL are already being used as surface heating for industrial applications in an unfocused area at very high power (even in the order of kilowatts when multiple modules are stacked). Further to this, during conventional SLM/EBM most heat produced during the process is lost from the surface of the powder bed leading to the development of high residual stresses within a component. Optical pre-heat may alleviate or completely eradicate this issue. Further work will need to assess whether melt pool formation/expansion was conduction limited or if generated temperatures were high enough to vaporise material and induce key-hole mode melting (possibly explaining the ability to process thicker powder layers with inclusion of large voids) [10].

The DAM process is highly scalable for the melting of larger areas in a single pass. DL bars consume a relatively small space and can be stacked easily to either cover a larger melting area or to superimpose laser beams such that the energy density per laser beam spot is increased. The higher wall plug efficiency of diode lasers together with the theoretically more efficient optical-to-thermal energy conversion at 808 nm has the potential to reduce energy consumption. However at this stage it is too early to claim DAM efficiency gains over conventional SLM/EBM approaches. Validation of this theoretical hypothesis requires confirmation through further experimental work. The wavelength tunability of diode lasers could be exploited to operate at the peak absorption wavelengths of different materials, even targeting different materials separately.

The current limitations of AM of metals systems (i.e. high purchase costs, high energy consumption and slow production time) may be overcome through the adoption of a diode laser module melting source. Previously, the use of low power diode bars for melting common SLM materials would be easily dismissed as being unable to provide the required energy density to melt these materials. This work has shown that this energy density challenge can be overcome and presents a first step in developing a novel and efficient high speed metallic additive manufacturing process.

Acknowledgements

The authors would like to acknowledge support from a UK Engineering & Physical Sciences Research Council (EP/K503812/1) IIKE Proof of

Concept award. Also acknowledge support from the Science and Technology National Council (CONACYT) of Mexico.

References

[1] M. Baumers, C. Tuck, R. Wildman, I. Ashcroft, E. Rosamond, R. Hague, Transparency built-in, J. Ind. Ecol. 17 (2013) 418–431.
[2] J.P. Bergmann, M. Bielenin, M. Stambke, T. Feustel, P.V. Witzendorff, J. Hermsdorf, Effects of diode laser superposition on pulsed laser welding of aluminum, Phys. Procedia 41 (2013) 180–189.
[3] D. Bergstrom, The Absorption of Laser Light by Rough Metal Surfaces - PhD Thesis, Lulea University of Technology, 2008.
[4] A. Ellis, C.J. Noble, N. Hopkinson, High speed sintering: assessing the influence of print density on microstructure and mechanical properties of nylon parts, Addit. Manuf. 1–4 (2014) 48–51.
[5] C. Emmelmann, M.F. Zaeh, T. Graf, M. Schmidt, J.P. Bergmann, M. Bielenin, M. Stambke, T. Feustel, P.V. Witzendorff, J. Hermsdorf, Lasers in manufacturing (LiM 2013) effects of diode laser superposition on pulsed laser welding of aluminum, Phys. Procedia 41 (2013) 180–189.
[6] S. Hengesbach, R. Poprawe, D. Hoffmann, M. Traub, T. Schwarz, C. Holly, F. Eibl, A. Weisheit, S. Vogt, S. Britten, M. Ungers, U. Thombansen, C. Engelmann, V. Mamuschkin, P. Lott, "Brightness and average power as driver for advancements in diode lasers and their applications", Proc. SPIE 9348, High-Power Diode Laser Technology and Applications XIII, 93480B, 2015.
[7] Y. Junhong, G. Linhui, W. Hualing, W. Zhao, T. Hao, G. Songxin, W. Deyong, Z. Kai, High brightness laser-diode device emitting 500 W from a 200 μm/NA0.22 fiber, Optics & Laser Technology 80 (2016) 92–97.
[8] H. Karstensen, R. Frankenberger, High-efficiency two lens laser diode to single-mode fiber coupler with a silicon plano convex lens, J. Lightwave Technol. 7 (1989) 244–249.
[9] K. Kellens, E. Yasa, R. Renaldi, W. Dewulf, J.P. Kruth, J. Duflou, Energy and Resource Efficiency of SLS/SLM Processes, 2011 (Solid Freeform Fabrication Symposium).
[10] W.E. King, H.D. Barth, V.M. Castillo, G.F. Gallegos, J.W. Gibbs, D.E. Hahn, C. Kamath, A.M. Rubenchik, Observation of keyhole-mode laser melting in laser powder-bed fusion additive manufacturing, J. Mater. Process. Technol. 214 (12) (2014) 2915–2925.
[11] A. Laskin, Applying of refractive spatial beam shapers with scanning optics, ICALEO 941-947 (2011).
[12] J.R. Lawrence, Advances in Laser Materials Processing: Technology, Elsevier Science, Research and Application, 2010.
[13] L. Li, The advances and characteristics of high-power diode laser materials processing, Opt. Lasers Eng. 34 (2000) 231–253.
[14] G. Manogharan, D. Soundararajan, R. Wysk, Study of Energy Efficiencies in Rapid Prototyping: EBM and CNC-RP. IIE Annual Conference. Proceedings, Institute of Industrial Engineers-Publisher, 2011 1.
[15] D. Miller, J. Bucklew, K. Enloe, D. Plourde, B. Lindahl, High Density Galvo Housing for Use with Multiple Laser Beams; Galvo System and Laser Beam Processing System with such Housing. EP20140193417, 2015.
[16] K.A. Mumtaz, N. Hopkinson, Selective laser melting of thin wall parts using pulse shaping, J. Mater. Process. Technol. 210 (2010) 279–287.
[17] K.A. Mumtaz, P. Vora, N. Hopkinson, A Method to Eliminate Anchors/Supports from directly Laser Melted Metal Powder Bed Processes, Solid freeform fabrication symposium, Austin, Texas, 2011.
[18] L.E. Murr, E. Martinez, K.N. Amato, S.M. Gaytan, J. Hernandez, D.A. Ramirez, P.W. Shindo, F. Medina, R.B. Wicker, Fabrication of metal and alloy components by additive manufacturing: examples of 3D materials science, J. Mater. Res. Technol. 1 (2012) 42–54.
[19] H. Nasim, Y. Jamil, Diode lasers: from laboratory to industry, Opt. Laser Technol. 56 (2014) 211–222.
[20] D. Schuöcker, Handbook of the EuroLaser Academy, Chapman & Hall, 1998.
[21] S.S. Sih, J.W. Barlow, The prediction of the emissivity and thermal conductivity of powder beds, Part. Sci. Technol. 22 (2004) 427–440.
[22] G.S. Sokolovskii, V.V. Dudelev, S.N. Losev, A.G. Deryagin, V.I. Kuchinskii, W. Sibbett, E.U. Rafailov, Superfocusing of mutimode semiconductor lasers and light-emitting diodes, Tech. Phys. Lett. 38 (2012) 402–404.
[23] V. Sturm, H.-G. Treusch, P. Loosen, Cylindrical Microlenses for Collimating High-Power Diode Lasers, 1997 717–726.
[24] S. Sumin Sih, J.W. Barlow, The prediction of the emissivity and thermal conductivity of powder beds, Part. Sci. Technol. 22 (2004) 291–304.
[25] I. Uk, Additive Manufacturing Special Interest Group - Shaping Our National Competency in Additive Manufacturing, 2012 (Technology Strategy Board).
[26] L.-L. Xiong, L. Cai, Y.-F. Zheng, H. Liu, P. Zhang, Z.-Q. Nie, X.-S. Liu, Slow axis collimation lens with variable curvature radius for semiconductor laser bars, Opt. Laser Technol. 77 (2016) 1–5.